Research on Definition of Short-Circuit Region for Γ-Source Circuit Breaker

Weizhang Song , Chen Wang , Ning An, Zhenhong Han, Dan Xue, and Patrick Wheeler , *Fellow, IEEE*

Abstract—This article proposes a method defining area of short-circuit and load step change for Γ-source circuit breaker through deriving the law between the variables of transformation ratio, coupling coefficient, load and the boundary resistance. First, the equivalent circuit as well as the steady-state and transient performance of Γ-source circuit breaker are analyzed. Then, the nonlinear segment equation of the boundary resistance for definition method through theoretical calculation and experimental data is fitted to avoid misoperation opening caused by load step change. Finally, the law between the transformer ratio, coupling coefficient, the load and the boundary resistance is obtained to define an accuracy short-circuit region. The feasibility and effectiveness of the proposed method have been verified using experimental results.

Index Terms—Short-circuit region definition, Z-source converter, Γ-source breaker.

I. Introduction

DC MICROGRID has attracted great attention due to its advantages of low line loss, strong stability, flexible power management, and low cost of transmission line construction [1]. Despite numerous advantages, fault protection remains a challenge restricting the extensive application of dc microgrids. The dc system must use special technical means to force the current to cross zero since there is no natural zero-crossing point, which causes the fault current rising rate very high and short-circuit protection very challenging [2], [3].

In order to solve the inherent problems of traditional circuit breakers and improve the protection performance of the dc system, in recent years, scholars have proposed a new type of dc circuit breaker—the Z-source DC circuit breaker [4]. Z-source circuit breaker mainly relies on the shoot-through mode of Z-source network to make thyristor achieve natural commutation to break short-circuit faults, and its the short-circuit protection does not require complex detection and control device, which not only improves the reliability of the system, but also can quickly break the short-circuit current [5], [6].

Therefore, the research of Z-source type dc solid-state circuit breakers have a broad development prospect. But it exists many defects such as not common ground between source and load, circulation, network resonance, etc. [7], [8], [9].

In order to overcome the inherent problems of Z-source type circuit breakers, many scholars have introduced coupled inductance to optimize and innovate the topology of Z-source circuit breaker, such as T-source circuit breaker [10], [11], reverse IT-source circuit breaker [12], Y-source circuit breaker [13], O-Z source circuit breaker [14] and IT-source circuit breaker [10]. In addition, for dc circuit breakers, besides topology performance, accurately identifying short-circuit faults and load step changes is a very important capability. However, in the current study, the turn-OFF region of Z-source circuit breaker are heavily dependent on circuit parameters, which limits the flexibility of the breakable area and may cause unexpected commutation of the thyristors due to the load step change, resulting in "misjudgment" [15], [16], [17]. Considering the limitation of the minimum fault slope rate, the turn-OFF region of Z-source circuit breaker was proposed in [18], [19], but its range is greatly affected by parameter. In [20], the equivalent circuit model of Z/T/IT-source circuit breakers were simplified and the internal connection between parameters was displayed through the 3-D map area, but the exact value of the failure area limit has not been given. Therefore, the turn-OFF region between the short-circuit fault and load step change becomes an urgent problem to be solved in the current Z-source type circuit breaker research.

The contribution of this article is to propose a method to define the turn-OFF region between short-circuit and load step change for the IT-source circuit breaker as well as explore its law between the three variables of transformation ratio, coupling coefficient, load and the boundary resistance. Meanwhile, the nonlinear segment equation of the boundary resistance for definition method through theoretical calculation and experimental data is fitted to avoid misoperation opening caused by load step change.

Weizhang Song, Chen Wang, Ning An, Zhenhong Han, and Dan Xue are with the School of Electrical Engineering, Xi'an University of Technology, Xi'an 710054, China (e-mail: swz@xaut.edu.cn; 1211911009@stu.xaut.edu.cn; 2180320025@stu.xaut.edu.cn; 2201920028@stu.xaut.edu.cn; 2211921153@stu.xaut.edu.cn).

Patrick Wheeler is with Power Electronics, Machines and Control Group, Global Director of the University of Nottingham's Institute of Aerospace Technology, University of Nottingham, 999020 Nottingham, U.K. (e-mail: pat.wheeler@nottingham.ac.uk).
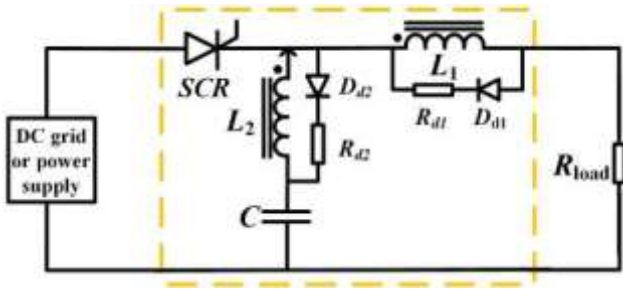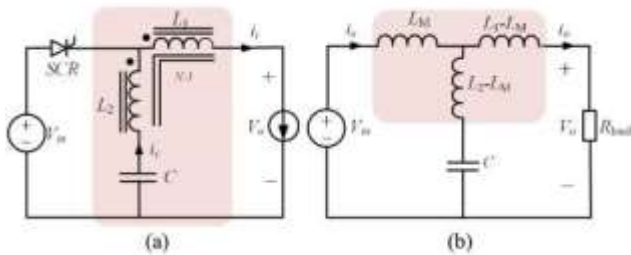
Fig. 1. Γ-source circuit breaker topology.

Fig. 2. Equivalent circuit diagram of Γ-source circuit breaker. (a) Nonshoot-through mode. (b) Steady-state equivalent circuit.

II. WORKING PRINCIPLES Γ-SOURCE CIRCUIT BREAKER

The steady-state and transient-state performance of the Γ-source circuit breaker are analyzed in this article. Fig. 1 is Γ-source circuit breaker topology, its working principles is to realize the breaking the fault by using its shoot-through operation mode, and to realize the normal power supply function by using its nonshoot-through operation mode.

A. The Steady-State Performance of Γ-Source Circuit Breaker

The steady-state performance determines the effect of the circuit breaker on the downstream load or converter. It can be seen from Fig. 2(a) that the Γ-source circuit breaker is in the non- shoot-through state and the thyristor *SCR* is turned-ON. Therefore, Γ-source circuit breaker realizes two functions under steady-state.

1) Energy storage: the power charges the capacitor C through the thyristor and the transformer secondary inductance L_2 to store energy for the short-circuit process.
2) Power supply to the load: the power supplies power to R_{load} through the thyristor and the primary side inductance L_1 of the transformer.

The transformer in the Γ-source circuit breaker is decoupled as shown in Fig. 2(b). And according to the mesh analysis for the equivalent circuit, write the loop equation in the complex frequency domain, as shown in

$$\begin{cases} L_M i_s s + (L_1 - L_M)i_o s + V_0 = V_{in} \\ V_0 = R_{load} i_o \\ (L_1 - L_M)i_o s + V_0 = \frac{1}{Cs}(i_s - i_o) + (L_2 - L_M)(i_s - i_o)s \end{cases}$$

Parameter				
Boundary resistance (Ω)	115.25	84.35	57.5	22.55
Transformer primary inductance (μH)	599	375	204	84
Transformer secondary inductance (μH)	26	26	26	26
Coupling coefficient k	0.766	0.70	0.869	0.725

TABLE II
PARAMETERS OF EXPERIMENT

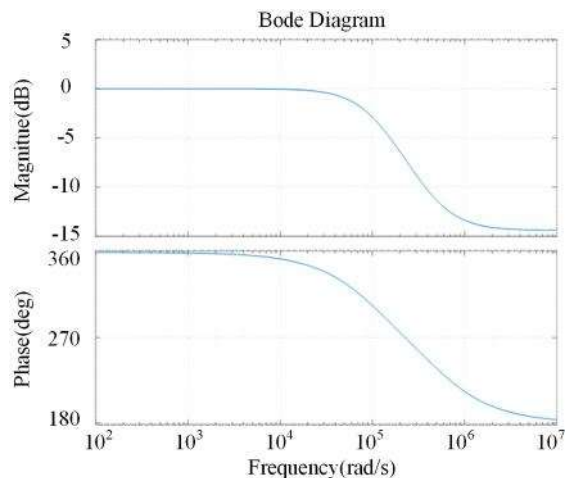| Parameter name	Parameter value
Input dc voltage	V_{in}=100 V
Transformer	L_1=599 μH L_2=26 μH N_1:N_2=48:10
Γ-source capacitance	C=100 μF
Load resistance	R_{load}=60 Ω

Fig. 3. Output-input voltage transfer function of Γ-source circuit breaker.

where i_s is the input current, i_o is the output current. V_{in} is the input voltage, V_o is the output voltage. L_M is mutual induction, and $L^2_m = L_1 * L_2$.

Combining the three equations in (1) to get the output-input voltage transfer function $G_v(s)$ of the Γ-source impedance network circuit, as shown in (2), which is used to analyze the filtering capability of the circuit breaker under the steady-state operation and the impact on the lower-level converter

$$G_v(s) = \frac{V_0}{V_{in}} = \frac{(L_2 - L_M)Cs^2 + 1}{L_2Cs^2 + \frac{L_1}{R_{load}}s + 1}. \tag{2}$$

Bring the experimental parameters in Table II into (2), the Bode diagram of this transfer function was drawn using MATLAB environment as shown in Fig. 3. It can be seen that at low frequencies, amplitude gain is 1 and the phase angle is zero, which indicates that the Γ-source circuit breaker can realize the energy transmission function during the steady-state; at the high
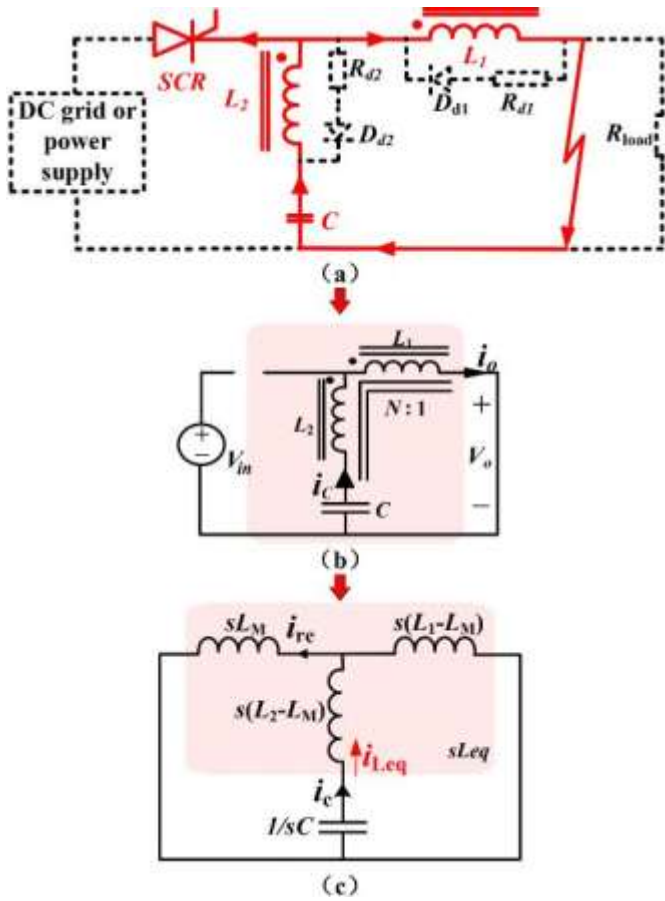
Fig. 4. Equivalent diagram of capacitor discharge and decoupling of Γ-source circuit breaker during turn-OFF state.

frequencies, starting at around $f = 10$ kHz, the amplitude gain is attenuated to -15 dB and the phase angle is attenuated to $180°$, which indicates that Γ-source circuit breaker has a low-pass filter characteristic and is especially suitable for active dc loads.

B. Transient-State Performance of Γ-Source Circuit Breaker

The Γ-source circuit breaker can break the short-circuit faults quickly and accurately, and its short-circuit equivalent circuit is shown in Fig. 4.

When the load is short-circuited, the capacitor C, the transformer secondary inductance L_2, the transformer primary inductance L_1 and the short-circuit point form a discharge circuit, as shown in Fig. 4(a). The noncoupling point of the transformer primary inductance L_1 and the coupling point of the transformer secondary inductance L_2 produce a forward voltage showing the relationship of the transformer ratio, so that the thyristor withstand the reverse voltage and produce a coupling current opposite to the normal load current on the primary side of the transformer, the current on the power-side begins to decrease. When the reverse coupling current is equal to the normal load current, the thyristor has a zero-crossing point, and the power and the load are switched-OFF naturally.

When the thyristor is turned-OFF, the dissipative branch without turning-ON is ignored, and the active load is equivalent

to a voltage source. Therefore, the Γ-source circuit breaker in Fig. 4(a) is further simplified as shown in Fig. 4(b).

The equivalent circuit of Fig. 4(b) is decoupled and equivalent to obtain Fig. 4(c), where L_M is the mutual inductance between the primary and secondary inductances.

With the capacitor as the port, the equivalent inductance of Γ-source circuit breaker is $(L_1\text{-}L_M)$ and L_M in parallel, and then connected in series with $(L_2\text{-}L_M)$, Finally, the equivalent inductance L_{eq} of the Γ-source circuit breaker is

$$L_{eq} = \frac{L}{L_1 L_2 - L_{2M}} \tag{3}$$

The current i_{SCR} flowing through the thyristor is the difference between the load current i_o and the reflected current i_{re}, where each current direction is indicated in Fig. 4. It can be calculated from Fig. 4(c) that the reflected current i_{re} is

$$i_{re} = \frac{L_1 - L_M i_c}{L_1} \tag{4}$$

where i_c is capacitive current.

When the load is short-circuited, the capacitor and coupled inductor produce resonance, then the capacitor current i_c is

$$i_c = i_{L_{eq}} = \frac{V_{in}}{\omega L_{eq}} \sin(\omega t) \tag{5}$$

where $\omega = \frac{1}{L_{eq}C}$, i_{Leq} is the current of the equivalent inductance of Γ-source circuit breaker.

Substituting (4) into (5), the current i_{re} reflected to the source side is

$$i_{re} = \frac{L_1 V_i C}{L_1} \frac{1}{L_{eq}} \sin \frac{1}{\sqrt{L_{eq}C}} t. \tag{6}$$

The thyristor currents is obtained as follows:

$$i_{scr} = \frac{V_{in} L_1 - L_M}{R_{load} \quad L_1} - \frac{C}{L_{eq}} V_{in} \frac{1}{\sqrt{L_{eq}C}} \sin t. \tag{7}$$

When the thyristor is turned-OFF, $i_{SCR} = 0$, then the time required for the zero-crossing point of the thyristor is

$$t = \sqrt{L_{eq}C} \arcsin \frac{L_1 \sqrt{A_N C}}{R_{load}(L_1 - L_M)C}. \tag{8}$$

Bring the data in Table II into (8) to calculate the turn-OFF time of the Γ-source circuit breaker. The results show that when a short-circuit fault occurs on the load-side, the zero-crossing time of the thyristor current of the Γ-source circuit breaker is 12 ìs, which proves that the Γ-source circuit breaker can break the fault quickly.

The process of the transformer current drops to zero is shown in Fig. 5. After the thyristor is turned-OFF, the capacitor resonates with the transformer inductance. When the capacitor voltage drops to zero, the buffer absorption circuit diode on the primary and secondary coupling inductors of the transformer conducts forward. The current decreases exponentially in the buffer absorption circuit, dissipating the energy stored in the transformer inductance in the form of heat on the resistance of the buffer
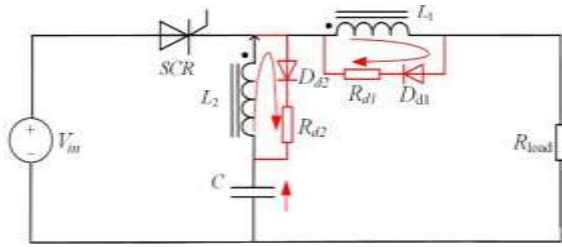
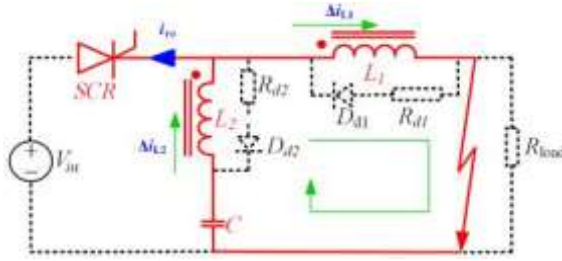Fig. 5. Inductive discharge process.

Fig. 6. Schematic diagram of current direction at the moment of short circuit.

absorption circuit until the current on the coupling inductance becomes zero.

III. Γ-DCCB SHORT-CIRCUIT AND LOAD STEP CHANGE AREA DEFINITION

The turn-OFF range of the circuit breaker, a key performance index of the circuit breaker, can demarcate the boundary resistance of the circuit breaker short-circuit fault and load step change. Taking the Γ-source circuit breaker as the research object, supposing the boundary resistance value of short-circuit and load step change is R_{bound} and the short-circuit resistance is R_{fault}, the actual turn-OFF area is jointly adjusted through theoretical derivation and simulation experiment.

A. Area Definition With Considering Fault Resistance

When $R_{fault} < R_{bound}$, the circuit has a short-circuit fault; when $R_{fault} \geq R_{bound}$, the circuit is normally powered. That is, R_{bound} is the boundary resistance value of short-circuit fault and load step change.

When the circuit is short-circuited, the current increment A_{iL2} of the transformer secondary inductance is equal to the capacitor current, and the direction of the primary inductance incremental current A_{iL1} is opposite to the load current in steady-state. When A_{iL1} increases to be equal to the steady-state current, the thyristor turns-OFF.

The current direction of A_{iL1}, A_{iL2} and the direction of the reflected current i_{re} are shown in Fig. 6.

Because turns-OFF speed of the thyristor very fast, the capacitive current increment can be approximated as the change of load current, expressed as

$$A_{iL1} = \frac{V_0 \cdot R_{fa} \cdot +4 1 \cdot i_{load}}{R_{fault} \cdot R_{load}} A_{iL2} = v,, R_{ft} + \frac{Rl^{f}{}_{,a}^{o}}{oad} \quad (9)$$

The relationship between the incremental current A_{iL1} and A_{iL2} and the transformation ratio N is

$$\frac{A_{iL1}}{A_{iL2}} = \frac{1}{N} \quad (10)$$

Putting (9) into (10), then

$$N \left(\frac{V_0 R_{fault} R_{load}}{R_{fault} \cdot R_{load}} - \frac{V_0}{R_{load}} \cdot 1 \right) = V_0 R_{fault} R_{load} . \frac{}{R_{fault} \cdot R_{load}} \quad (11)$$

It can be obtained by simplifying (11)

$$R_{bound} = (N - 1)R_{load}. \quad (12)$$

It can be seen that the boundary resistance is proportional to the load resistance R_{load}, and has linear relationship with the transformation ratio N of the transformer.

Establish (13) based on the relationship between the transformation ratio and the reverse current of the thyristor is greater than the load current. Combining (10) with (12), a 3-D diagram is drawn as shown in Fig. 6, which represents the change trend and peak limit between the three variables of the transformer ratio N, the load resistance R_{load} and the boundary resistance R_{bound}

$$A_{iL1} > \frac{N_2}{N_1 - N_2} i_o \quad (13)$$

where N_1 is the number of coil turns on the primary side of the transformer and N_2 is the number of coil turns ON the secondary side of the transformer.

The red area in Fig. 7 represents the ability to achieve turn-OFF area ($i_s < 0$), the blue area represents the inability to achieve turn-OFF area ($i_s \geq 0$), and the boundary resistance between the two is the boundary resistance value. It can be seen from Fig. 6 that when the load is constant, the area that can be turned-OFF increases as the transformer ratio increases, when the transformer ratio is constant, the area that can be turned-OFF increases as the load increases. therefore, the short-circuit turn-OFF area can be controlled by constraining the transformer ratio and the load.

In summary, with the increase of the transformation ratio, the range of turn-OFF increases and the allowable load step change range decreases, which may cause false turn-OFF. Therefore, it is necessary to adjust the transformation ratio to regulate the short-circuit turn-OFF area according to the load, allowable overload limit and the switch-OFF range.

B. Area Definition With Considering Leakage Inductance

The core of the coupled circuit breaker is that the magnetic coupling generates reverse current to naturally commutate the thyristor, so the influence of the transformer leakage inductance on the definition of the short-circuit and load step change area must be considered. Fig. 8 is a hyperbolic diagram of the theoretically boundary value and the simulated boundary value when the leakage inductance of the transformer is considered and when $R_{load} = 60 \ \Omega$. When the transformer ratio N is less than 7, the theoretical value is consistent with the simulated value; when N is more than 7, the actual boundary resistance no longer increases linearly, and the error between the theoretical value and the simulated value becomes larger and larger. It can
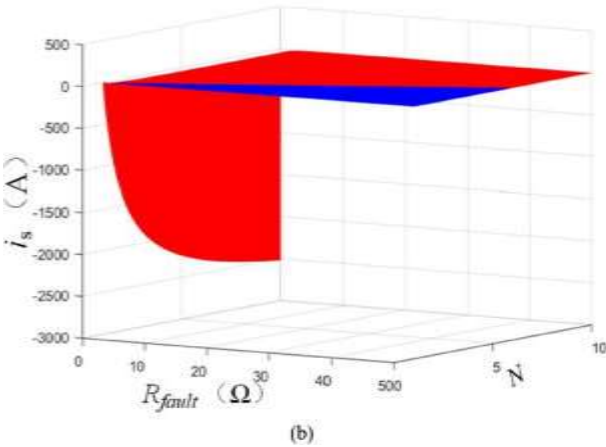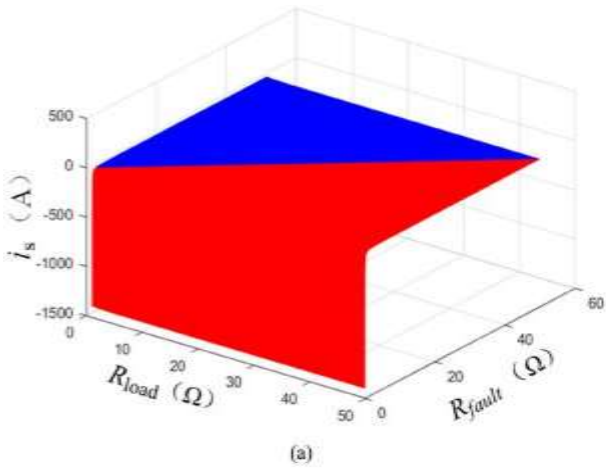
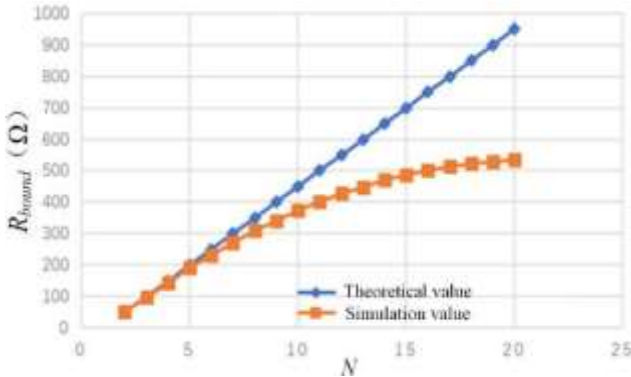Fig. 7. Trend of input current under different parameters. (a) $N = 2$. (b) R_{load} = 60 Ω.

Fig. 8. Short-circuit and load step change boundaries when considering transformer leakage inductance.

be shown that when the transformation ratio is within a certain range, the leakage inductance has influence on the boundary resistance value.

C. Area Definition With Considering Coupling Coefficient

In order to define the boundary resistance more accurately, this article considers the influence of the coupling coefficient
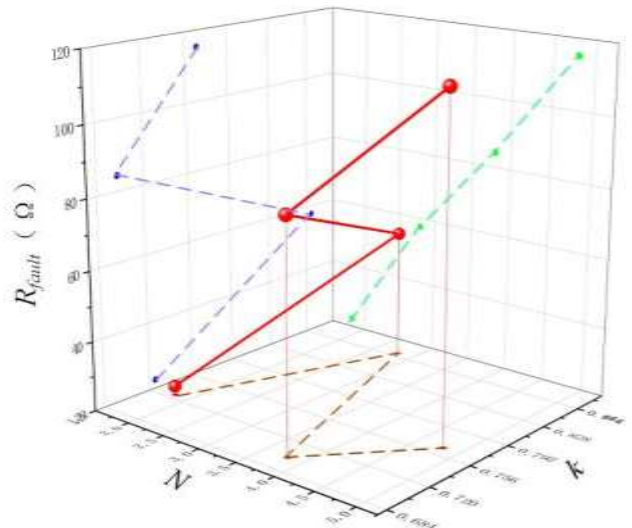

Fig. 9. Broken line chart (the red line) of boundary resistance under different transformation ratios and coupling coefficients (the three dotted lines are the projections of the red line on the *xoy, xoz*, and *yoz* planes, respectively.).

k of the transformer, and designs transformers with different transformation ratios and different coupling coefficients for experiments. The specific parameters are given in Table I.

According to the transformer ratio, boundary resistance and coupling coefficient in Table I, Fig. 9 (i.e., red broken line) is drawn, which is in an "oblique Z" shape, and the three dotted lines are projected on the *xoy, xoz*, and *yoz* planes, respectively.

It can be seen that when the coupling coefficient is constant, the boundary resistance increases nonlinearly with the transformer ratio; when the transformer ratio is constant, the boundary resistance presents an "inverted Z" shape with the coupling coefficient, as shown by the blue dotted line on the *yoz* plane. Therefore, considering the coupling coefficient is necessary to define the boundary resistance between short-circuit and load step change.

Through several breaking experiments, the breaking data of the load side faults of the Γ-source circuit breaker are recorded and sorted out, the numerical analysis of multiple groups of data is carried out by MATLAB, and the boundary resistance equation of the piecewise function is regulated again. The boundary resistance equation can be further modified as

$$R_{bound} =$$

$$\begin{cases} 0.45(N-1)R_{load}e^{\square K/k} & 0 < N < 7, 0 < k < 1 \\ 4.77R_{load}e^{-\square(N-\square)^2+\square} & N \sim 7, 0 < k < 1. \end{cases} (14)$$

D. Three-Dimensional Map of Area Definition

In order to more intuitively express the peak change relationship between the boundary resistance and the transformation ratio, coupling coefficient, load resistance of the transformer. The control variable method is used to reduce the dimensionality and the boundary resistance is drawn through the 3-D graph in this article.
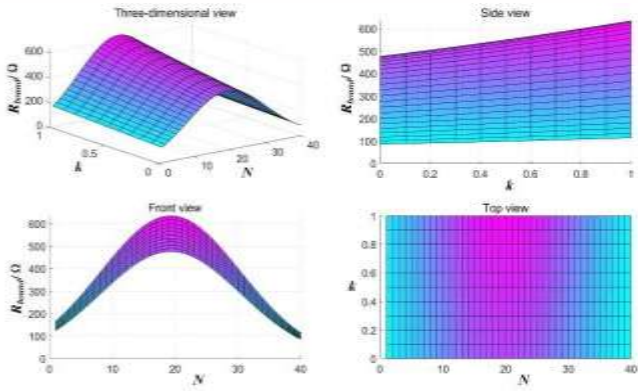
Fig. 10. Three views of the boundary resistance when $R_{load} = 100\ \Omega$.

Fig. 11. Block diagram of Bi-Γ-source circuit breaker system implementation.

Analyzing (14), the load resistance R_{load} does not affect the curved surface trend of the boundary resistance value of load short circuit and load step change, but only affects the slope change of the curved surface. The smaller the resistance value of the load resistance, the smoother the curved surface.

Fig. 10 shows the 3-D curved surface diagram of the transformer transformation ratio, coupling coefficient and boundary resistance when R_{load} = 100 Ω. According to the analysis of the side view and front view, the boundary resistance shows a parabolic change (increases and then decreases) with the increase of the transformer ratio, and slowly increase with the coupling coefficient increases, and there is a peak value at N = 19.3, and the boundary resistance R_{bound} = 635 Ω at this time. Therefore, Fig. 10 not only show the change trend and peak limit of complex parameters, but also provide the direction and theoretical basis for the experiment and practical application of the subsequent design of Π-source circuit breaker.

Based on the above analysis, several rules about the turn-OFF region between short-circuit and load step change for the Π-source circuit breaker are summarized as follows.

1) Boundary resistance value R_{bound} of judging short-circuit or load step change is related to transformation ratio N, coupling coefficient k, the load resistance R_{load}.
2) Boundary resistance value R_{bound} is proportional to the load resistance R_{load}.
3) Boundary resistance value R_{bound} shows a trend of increases first and then decreases with the increase of the transformer ratio N.
4) Boundary resistance value R_{bound} shows a slowly increase with the coupling coefficient k increases.

IV. EXPERIMENTAL VERIFICATION AND ANALYSIS

In order to verify the effectiveness of the short-circuit and load step change region definition of the Π-source circuit breaker model, an experimental platform for the main circuit of the Π-source dc solid-state circuit breaker was built, and a control core based on TMS320F2812 DSP was used. The system block diagram and experimental prototype are shown in Figs. 11 and 12. The experimental parameters and device models are given in Tables II and III.
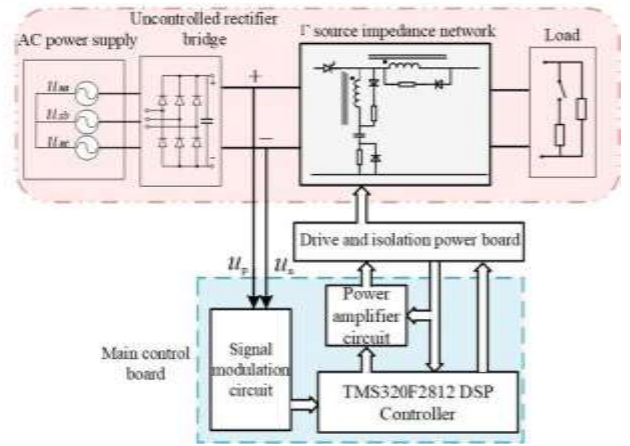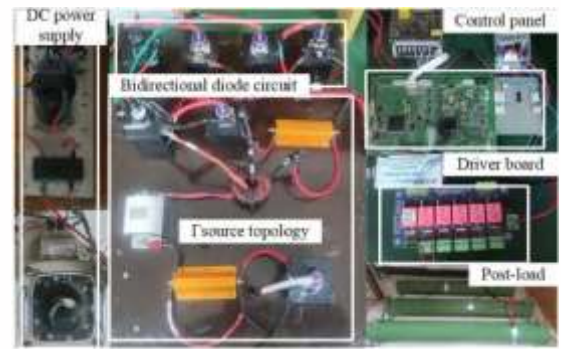

Fig. 12. Experimental platform.

TABLE III
DEVICE TABLE

Transformer	T250-52	Primary inductance		Secondary inductance	
		548 µH		24.8 µH	
Capacitance	CBB16	Capacity range		Withstand voltage	
		100 µF		800 V	
thyristor	KG30A	V_{RRM}/V_{DRM}	$I_{T(AV)}$	I_{TSM}	
		100/1800 V	30 A	390 A	
Diode of snubber circuit	KP30A	V_{RRM}/V_{DRM}	$I_{T(AV)}$	I_{TSM}	
		100/2000 V	5 A	390 A	
Resistance of snubber circuit	RX24-200W-5ΩJ	Rated power		Resistance	
		200 W		50 Ω	

A. Function Analysis of Π-Source Breaker in Steady-State

Fig. 13 shows the experimental waveforms of capacitor voltage, thyristor voltage, load voltage and load current when the Π-source circuit breaker is in steady-state. It can be seen that, in steady-state, the power charges the capacitor to realize energy storage, and the power, thyristor and primary-side inductance of transformer supply power to the load. At this time, the voltage of the load is approximately equal to voltage of the power.
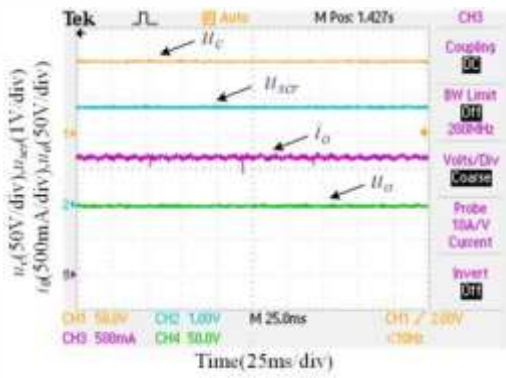
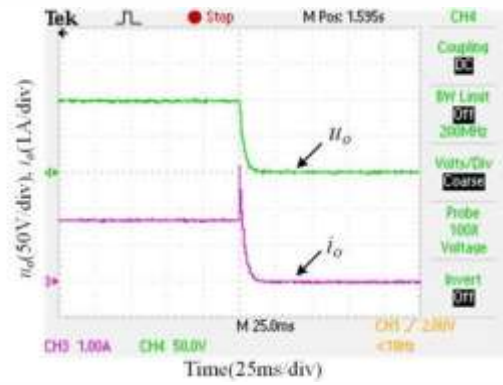Fig. 13. Steady-state waveform of the Γ-source breaker.

Fig. 16. Voltage and current waveforms on the load-side in short-circuit state.
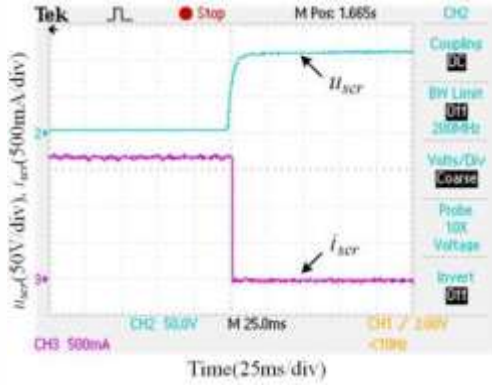

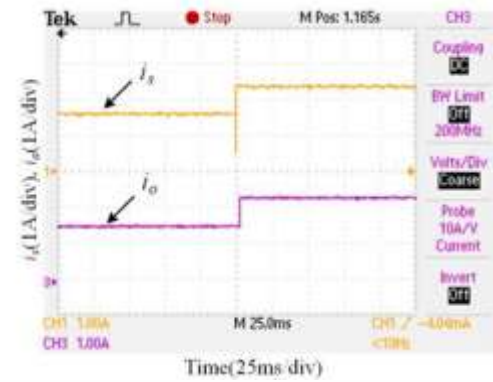Fig. 14. Voltage and current waveforms of thyristor in short-circuit.

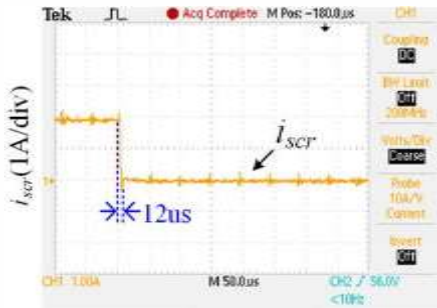Fig. 17. Power-side and load-side current during overload.

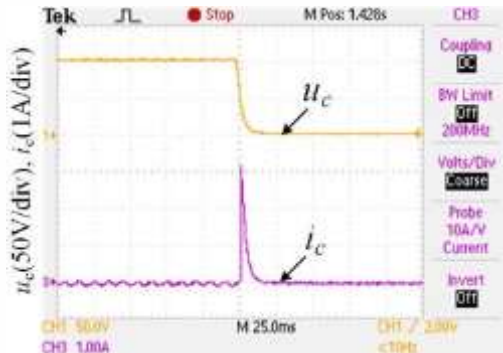Fig. 15. Enlarged diagram of the turn-OFF time of the thyristor.

Fig. 18. Voltage and current waveforms of capacitor during short-circuit.

It is verified that IT-source circuit breaker can realize energy transmission function in steady-state.

*B. Function Analysis of IT-Source Breaker in Transient State*

Figs. 14 and 16 show the voltage and current waveforms of thyristor and the load-side of IT-source circuit breaker in short-circuit state. When short-circuit fault occurs, the thyristor current quickly drops to zero, effectively breaking the short-circuit fault; the thyristor voltage rises to the power-side voltage, and the forward blocking characteristic of the thyristor is restored; the voltage and current on the load-side drop to zero momentarily, which breaks the power and the load, ensuring the safety of the system. The effectiveness of the IT-source circuit breaker breaking short-circuit fault is verified.

Among them, the enlarged diagram of the turn-OFF time of the thyristor is shown in Fig. 15, which is consistent with the simulation results and theoretical derivation, and can verify its microsecond level turn-OFF speed.

Fig. 17 shows the current waveforms on the power-side and the load-side when the IT-source circuit breaker is overloaded by 25%. It can be seen that the power-side current first decreases and then increases to a steady value, and the power-side current steps to another steady value that equal to the load current. It shows that IT-source circuit breaker can withstand a certain load step change.
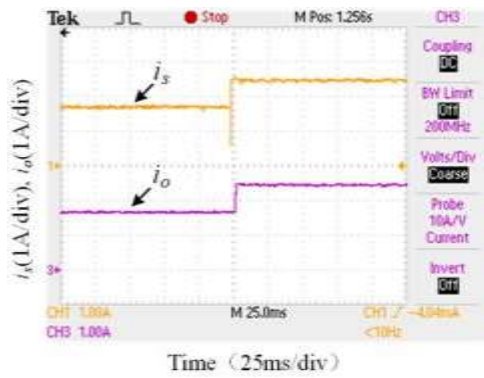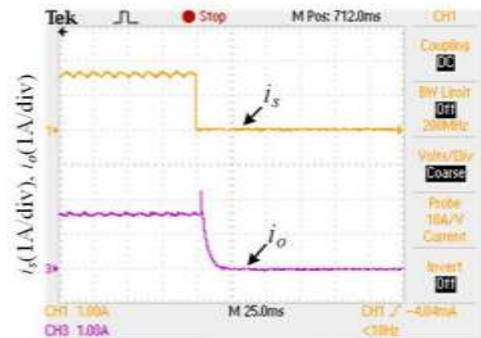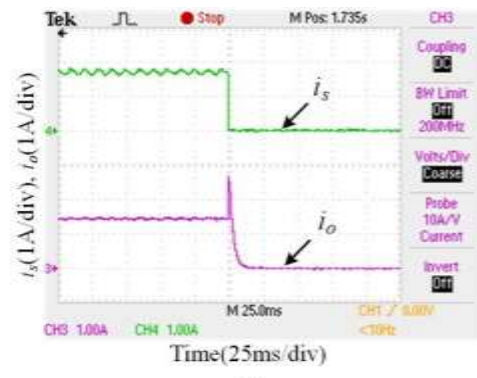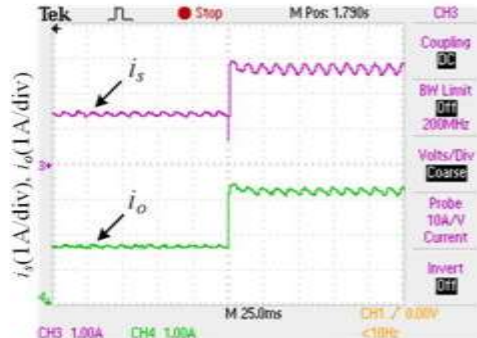
Fig. 19. Current waveforms on the power-side and the load-side when N = 4.8, k = 0.766. (a) R_{fault} = 117 . (b) R_{fault} = 113.5 .

Fig. 21. Power- side and load current waveforms when N = 2.8, k = 0.869. (a) R_{fault} = 56.5 . (b) R_{fault} = 58.5.
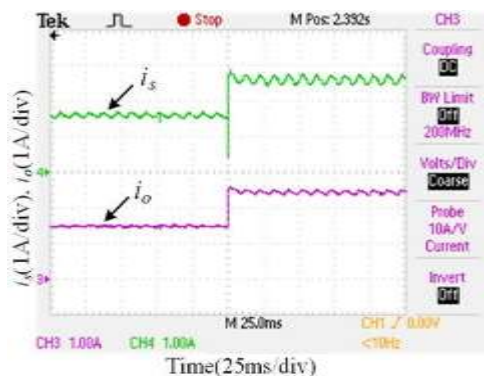

Fig. 20. Current waveforms on the power-side and the load-side when N = 3.8, k = 0.7. (a) R_{fault} = 83 . (b) R_{fault} = 85.7 .

Fig. 18 shows experimental waveforms of capacitor voltage and current during short-circuit. It can be seen that during short-circuit, the voltage capacitor drops to zero due to capacitor discharge. At same time, the capacitor current sharply increases and a peak appears, which is coupled by the primary inductance of transformer to generate a reverse current that forces the thyristor to cross zero and turn-OFF. This verifies the feasibility of the capacitor cooperating with the transformer's equivalent inductance to force the thyristor to break the faults when Γ-source circuit breaker is short-circuited.

C. Experiment Analysis of Area Definition

In order to verify accuracy of the turn-OFF range of the short-circuit and load step change, the experimental is implemented with different transformer ratios N and coupling coefficients k.

Set N = 4.8, k = 0.766, the current waveforms on the power-side and the load-side are shown in Fig. 19. When R_{fault} is set to 117 1, the current on the power-side decreases, but the reflected current i_{re} is always smaller than the normal load current, the thyristor is still ON, so the circuit breaker fails to turn-OFF; when R_{fault} is set to 113.5 1, the current on the power-side and the load-side current drops to zero instantly, realizing the faults breaking. Therefore, it can be judged that the range of the boundary resistance is 113.5–117 1, and R_{bound} = 115.25 1 is obtained by squeeze theorem.

Set N = 3.8, k = 0.7, the current of power-side and load-side experimental waveforms are shown in Fig. 20. When R_{fault} is set to 85.7 1, the current on the power-side decreases, but the reflected current i_{re} is always smaller than the normal load current, the thyristor is still ON, so the circuit breaker fails to turn-OFF; when R_{fault} is set to 83 1, the current on the power-side and the load-side current drops to zero instantaneously, realizing the faults breaking. It can be seen that the range of the boundary resistance is 83–85.7 1. According to squeeze theorem, the fault boundary resistance R_{bound} = 84.35 1.

Set N = 2.8, k = 0.869, the current of power-side and load-side experimental waveforms are shown in Fig. 21. When R_{fault} is
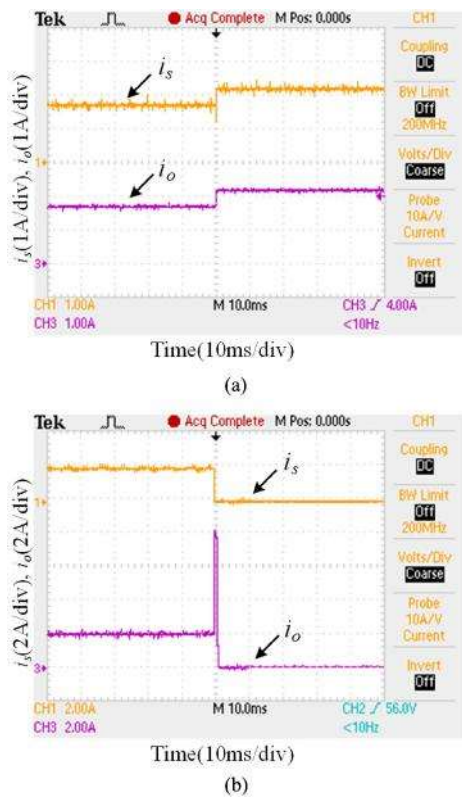
Fig. 22. Current waveforms on the power-side and the load-side when $N = 19.3$ and $k = 0.8$. (a) $R_{\tt fault} = 352$. (b) $R_{\tt fault} = 348$.

Transformation ratio	Theoretical value [calculated according to formula(14)]	Experimental value	Error
48:10; and $k = 0.766$	127 Ω	115.25 Ω	9%
38:10; and $k = 0.7$	92 Ω	84.35 Ω	8%
28:10; and $k = 0.869$	62 Ω	57.5 Ω	7%
193:10; and $k = 0.8$	360 Ω	350 Ω	2%

V. CONCLUSION

This article proposes a method to define the turn-OFF region between short-circuit and load step change for the IT-source circuit breaker as well as explores its law between the variables of transformation ratio, coupling coefficient, the load, and the boundary resistance. The experimental results show that: IT-source circuit breaker can realize low-pass filter function in steady-state and quickly break the faults in short-circuit state as well as has a good circuit breaker functional characteristics; and an accuracy definition the turn-OFF region between short-circuit and load step change is obtained to avoid misoperation regardless of the short-circuit and load step change. Finally, under the changes of different influencing factors, the experimental delimited values of the short-circuit and load step change area of IT-source circuit breaker are consistent with the theoretical delimited values.

set to 61.2 and 58.5 1, the current on the power-side decreases, but the reflected current $_{ire}$ is always smaller than the normal load current, the thyristor is still ON, so the circuit breaker fails to turn-OFF; when $_{Rfault}$ is set to 56.5 and 54 1, the current on the power-side and the load-side current drops to zero instantaneously, realizing the faults breaking. According to squeeze theorem, the fault boundary resistance $R_{\bf bound} = 57.5$ 1.

Set $N = 19.3$, $k = 0.8$, the current of power-side and load-side experimental waveforms are shown in Fig. 22. When $_{Rfault}$ is set to 360 and 352 1, the current on the power-side decreases, but the reverse coupling current is always smaller than the normal load current, the thyristor is always in the on state, and the turn-OFF fails; when $_{Rfault}$ is set to 348 and 340 1, the current on the power-side and the load-side current drops to zero instantaneously, realizing fault turn-OFF. At this time, the boundary resistance $R_{\bf bound} = 350$ 1is obtained by the clamping criterion, which verifies accuracy of the self-shutdown failure area definition scheme of IT-source circuit breaker.

The theoretical values calculated by (14) and the conclusions obtained from the experiment are given in Table IV.

The above experiments have verified the boundary resistance of short-circuit and load step change of the IT-source circuit breaker under different parameter conditions. The experimental results are close to the theoretical calculation value, which verifies the effectiveness of the self-shutdown failure area definition of IT-source circuit breaker, and which verifies the theoretical accuracy of the shutdown bound of IT-source circuit breaker.

REFERENCES

[1] S. Zheng, R. Kheirollahi, J. Pan, L. Xue, J. Wang, and F. Lu, "DC circuit breakers: A technology development status survey," *IEEE Trans. Smart Grid*, vol. 13, no. 5, pp. 3915–3928, Sep. 2022.

[2] K. K. M. Siu, C. N. M. Ho, and D. Li, "Design and analysis of a bidirectional hybrid DC circuit breaker using AC relays with long life time," *IEEE Trans. Power Electron.*, vol. 36, no. 3, pp. 2889–2900, Mar. 2021.

[3] Y. Guo, G. Wang, D. Zeng, H. Li, and H. Chao, "A thyristor full-bridge-based DC circuit breaker," *IEEE Trans. Power Electron.*, vol. 35, no. 1, pp. 1111–1123, Jan. 2020.

[4] K. A. Corzine and R. W. Ashton, "A new Z-source DC circuit breaker," in *Proc. IEEE Int. Symp. Ind. Electron.*, 2010, pp. 585–590.

[5] R. Rodrigues, Y. Du, A. Antoniazzi, and P. Cairoli, "A review of solid-state circuitbreakers,"*IEEETrans. PowerElectron.*,vol. 36,no. 1,pp. 364–377, Jan. 2021.

[6] A. Maqsood, A. Overstreet, and K. A. Corzine, "Modified Z-source DC circuit breaker topologies," *IEEE Trans. Power Electron.*, vol. 31, no. 10, pp. 7394–7403, Oct. 2016.

[7] Y. Yang and C. Huang, "A low-loss Z-source circuit breaker for LVDC systems," *IEEE J. Emerg. Sel. Topics Power Electron.*, vol. 9, no. 3, pp. 2518–2528, Jun. 2021.

[8] S. G. Savaliya and B. G. Fernandes, "Analysis and experimental validation of bidirectional Z-source DC circuit breakers," *IEEE Trans. Ind. Electron.*, vol. 67, no. 6, pp. 4613–4622, Jun. 2020.

[9] D. J. Ryan, H. D. Torresan, and B. Bahrani, "A bidirectional series Z-source circuit breaker," *IEEE Trans. Power Electron.*, vol. 33, no. 9, pp. 7609–7621, Sep. 2018.

[10] Z. Zhou, J. Jiang, S. Ye, C. Liu, and D. Zhang, "A Γ-source circuit breaker for DC microgrid protection," *IEEE Trans. Ind. Electron.*, vol. 68, no. 3, pp. 2310–2320, Mar. 2021.

[11] L. Changle, N. Ziling, and Z. Junjie, "Research on new T-source DC solid-state circuit breaker technology," *Proc. Chin. Soc. Elect. Eng.*, vol. 38, no. 3, pp. 879–889, Feb. 2021.

[12] H. Al-Khafaf and J. Asumadu, "T-Z-source DC circuit breaker operation with variable coupling coefficient k," in *Proc. IEEE Int. Conf. Electro Inf. Technol.*, 2017, pp. 492–496.

[13] Y. Wang, W. Li, X. Wu, and X. Wu, "A novel bidirectional solid-state circuit breaker for DC microgrid," *IEEE Trans. Ind. Electron.*, vol. 66, no. 7, pp. 5707–5714, Jul. 2019.

[14] Z. Zhou, J. Jiang, S. Ye, D. Yang, and J. Jiang, "Novel bidirectional O-Z-source circuit breaker for DC microgrid protection," *IEEE Trans. Power Electron.*, vol. 36, no. 2, pp. 1602–1613, Feb. 2021.

[15] K. A. Corzine, "A new-coupled-inductor circuit breaker for DC applications," *IEEE Trans. Power Electron.*, vol. 32, no. 2, pp. 1411–1418, Feb. 2017.

[16] J.-D. Park, J. Candelaria, L. Ma, and K. Dunn, "DC ring-bus microgrid fault protection and identification of fault location," *IEEE Trans. Power Del.*, vol. 28, no. 4, pp. 2574–2584, Oct. 2013.

[17] Y. Wang, Y. Li, A. Junyent-Ferré, and M. Kim, "H5+ converter: A bidirectional AC–DC converter with DC-fault-blocking and self-precharge capabilities," *IEEE Trans. Power Electron.*, vol. 34, no. 11, pp. 10619–10634, Nov. 2019.

[18] D. Keshavarzi, T. Ghanbari, and E. Farjah, "A Z-source-based bidirectional DC circuit breaker with fault current limitation and interruption capabilities," *IEEE Trans. Power Electron.*, vol. 32, no. 9, pp. 6813–6822, Sep. 2017.

[19] X. Zeng, K. Yu, Y. Wang, and Y. Xu, "A novel single phase grounding fault protection scheme without threshold setting for neutral ineffectively earthed power systems," *Comput. Sci. Elect. Eng. J. Power Energy Syst.*, vol. 2, no. 3, pp. 73–81, Sep. 2016.

[20] X. Diao, F. Liu, Y. Song, M. Xu, Y. Zhuang, and X. Zha, "Topology simplification and parameter design of Z/T/Γ-source circuit breakers," *IEEE J. Emerg. Sel. Topics Power Electron.*, vol. 9, no. 6, pp. 7066–7077, Dec. 2021.

Ning An was born in Shaanxi, China, in 1996. She received the B.S. and M.S. degrees in electrical engineering from the Xi'an University of Technology, Xi'an, China, in 2018 and 2021, respectively.

Zhenhong Han was born in Shandong, China, in 1998. He received the B.S. degree in electrical engineering from the Xi'an University of Technology, Xi'an, China, in 2020. Heis currently working toward the M.S. degree in electrical engineering with the School of Electrical Engineering, Xi'an University of Technology, Xi'an, China.

His current research interests include dc solid-state circuit breaker.

Dan Xue was bornin Shaanxi, China, in 1999. Shereceived the B.S. degree in electrical engineering from the Xi'an University of Technology, Xi'an, China, in 2021. She is currently working toward the M.S. degree in electrical engineering with the School of Electrical Engineering, Xi'an University of Technology, Xi'an, China.

Her current research interests include dc solid-state circuit breakers, and dc microgrid protection system.

Patrick Wheeler (Fellow, IEEE) received the B.Eng. (Hons.) and Ph.D. degrees in electrical engineering from the University of Bristol, Bristol, U.K., in 1990 and 1994, respectively.

He is currently the Head of the Power Electronics, Machines and Control Group, Global Director of the University of Nottingham's Institute of Aerospace Technology and was the Li Dak Sum Chair Professor in Electrical and aerospace engineering. He has authored or coauthored more than 750 academic publications in leading international conferences and journals.

Weizhang Song was born in Henan, China, in 1980. He received the B.S. and M.S. degrees in information and control engineering, and the Ph.D. degree in electrical engineering from the Xi'an University of Technology, Xi'an, China, in 2004, 2007, and 2010, respectively.

From 2014 to 2015, he was a Research Fellow with the Power Electronics, Machines and Control Group, The University of Nottingham, Nottingham, U.K. He is currently aProfessor and the Vice President with the School of Electrical Engineering, Xi'an University Technology. He has authored or coauthored more than 60 refereed journal and international conference papers. His current research interests include power electronics, and ac drive system, in particular Z-source type dc circuit breaker, matrix converter and VIENNA rectifier.

Chen Wang was born in Beijing, China, in 1995. She received theB.S. degreeinelectrical engineering, and the M.S. degree in control theory and control engineering from the Xi'an Technological University, Xi'an, China, in 2017 and 2021, respectively. She is currently working toward the Ph.D. degree in electrical engineering with the School of Electrical Engineering, Xi'an University of Technology, Xi'an, China.

Her research interests include solid-state circuit breaker and DC microgrid protection system.